IOP PUBLISHING CLASSICAL AND QUANTUM GRAVITY

Class. Quantum Grav. **25** (2008) 114029 (9pp) doi:10.1088/0264-9381/25/11/114029

A coherent method for detection of gravitational wave bursts

S Klimenko[1], I Yakushin[2], A Mercer[1] and G Mitselmakher[1]

[1] University of Florida, PO Box 118440, Gainesville, FL 32611, USA
[2] LIGO Livingston Observatory, PO Box 940, Livingston, LA 70754, USA

Received 21 November 2007, in final form 28 February 2008
Published 15 May 2008
Online at stacks.iop.org/CQG/25/114029

Abstract
We describe a coherent network algorithm for detection and reconstruction of gravitational wave bursts. The algorithm works for two and more arbitrarily aligned detectors and can be used for both all-sky and triggered burst searches. We describe the main components of the algorithm, including the time-frequency analysis in a wavelet domain, construction of the likelihood time-frequency maps, and identification and selection of burst events.

PACS numbers: 04.80.Nn, 07.05.Kf, 95.30.Sf, 95.85.Sz

(Some figures in this article are in colour only in the electronic version)

1. Introduction

Coherent network analysis addresses the problem of detection and reconstruction of gravitational waves (GW) with networks of detectors. It has been extensively studied in the literature [1–6] in application to detection of bursts signals, which may be produced by numerous gravitational wave sources in the Universe [7–15]. In coherent methods, a statistic is built up as a coherent sum over detector responses. In general, it is expected to be more optimal (better sensitivity at the same false alarm rate) than the detection statistics of the individual detectors that make up the network. Also, coherent methods provide estimators for the GW waveforms and the source coordinates in the sky.

The method we present (called coherent WaveBurst) is significantly different from the traditional burst detection methods. Unlike coincident methods [16–18], which first identify events in individual detectors by using an excess power statistic and then require coincidence between detectors, the coherent WaveBurst method combines all data streams into one coherent statistic constructed in the framework of the constrained maximum likelihood analysis [4]. Such an approach has significant advantages over the coincident methods. First, the sensitivity of the method is not limited by the least sensitive detector in the network. In the coherent WaveBurst method, the detection is based on the maximum likelihood ratio statistic which represents the total signal-to-noise ratio of the GW signal detected in the network. Second, other coherent statistics, such as the null stream and the network correlation coefficient, can

be constructed to distinguish genuine GW signals from the environmental and instrumental artifacts. Finally, the source coordinates of the GW waveforms can be reconstructed.

2. Coherent analysis

The coherent WaveBurst pipeline (cWB) uses a method, for coherent detection and reconstruction of burst signals, based on the use of the likelihood ratio functional [4]. For a general case of Gaussian quasi-stationary noise, it can be written in the wavelet (time-frequency) domain as

$$\mathcal{L} = \sum_{k=1}^{K} \sum_{i,j=1}^{N} \left(\frac{w_k^2[i,j]}{\sigma_k^2[i,j]} - \frac{(w_k[i,j] - \xi_k[i,j])^2}{\sigma_k^2[i,j]} \right), \tag{1}$$

where K is the number of detectors in the network, $w_k[i,j]$ is the sampled detector data (time i and frequency j indices run over some time-frequency area of size N) and $\xi_k[i,j]$ are the detector responses. Note that we omit the term $1/2$ in the conventional definition of the likelihood ratio. The detector noise is characterized by its standard deviation $\sigma_k[i,j]$, which may vary over the time-frequency plane. The detector responses are written in the standard notations

$$\xi_k[i,j] = F_{+k} h_+[i,j] + F_{\times k} h_\times[i,j], \tag{2}$$

where $F_{+k}(\theta,\phi)$, $F_{\times k}(\theta,\phi)$ are the detector antenna patterns (depend upon source coordinates θ and ϕ) and $h_+[i,j]$ and $h_\times[i,j]$ are the two polarizations of the gravitational wave signal in the wave frame. Since the detector responses ξ_k are invariant with respect to the rotation around the z-axis in the wave frame, the polarization angle is included in the definition of h_+ and $h_\times$. The GW waveforms, h_+ and $h_\times$, are found by a variation of $\mathcal{L}$. The maximum likelihood ratio statistic is obtained by the substitution of the solutions into the functional $\mathcal{L}$. The waveforms in the time domain are reconstructed from the inverse wavelet transformation. Below, for convenience we introduce the data vector $\mathbf{w}[i,j]$ and the antenna pattern vectors $\mathbf{f}_+[i,j]$ and $\mathbf{f}_\times[i,j]$:

$$\mathbf{w}[i,j] = \left(\frac{w_1[i,j]}{\sigma_1[i,j]}, \ldots, \frac{w_K[i,j]}{\sigma_K[i,j]} \right) \tag{3}$$

$$\mathbf{f}_{+(\times)}[i,j] = \left(\frac{F_{1+(\times)}}{\sigma_1[i,j]}, \ldots, \frac{F_{K+(\times)}}{\sigma_K[i,j]} \right). \tag{4}$$

Further in the text, we omit the time-frequency indices and replace the sum $\sum_{i,j=1}^{N}$ with $\sum_{\Omega_{\mathrm{TF}}}$, where Ω_{TF} is the time-frequency area selected for the analysis.

The likelihood functional (equation (1)) can be written in the form $\mathcal{L} = \mathcal{L}_+ + \mathcal{L}_\times$:

$$\mathcal{L}_+ = \sum_{\Omega_{\mathrm{TF}}} \left[2(\mathbf{w} \cdot \mathbf{f}_+) h_+ - |\mathbf{f}_+|^2 h_+^2 \right], \tag{5}$$

$$\mathcal{L}_\times = \sum_{\Omega_{\mathrm{TF}}} \left[2(\mathbf{w} \cdot \mathbf{f}_\times) h_\times - |\mathbf{f}_\times|^2 h_\times^2 \right], \tag{6}$$

where the antenna pattern vectors $\mathbf{f}_+$ and $\mathbf{f}_\times$ are defined in the dominant polarization wave frame (DPF) [4]. In this frame, the antenna pattern vectors are orthogonal to each other: $(\mathbf{f}_+ \cdot \mathbf{f}_\times) = 0$. The estimators of the GW waveforms are the solutions of the equations

$$(\mathbf{w}\cdot\mathbf{f}_+) = |\mathbf{f}_+|^2 h_+, \tag{7}$$

$$(\mathbf{w}\cdot\mathbf{f}_\times) = |\mathbf{f}_\times|^2 h_\times. \tag{8}$$

Note that the norms $|\mathbf{f}_+|^2$ and $|\mathbf{f}_\times|^2$ characterize the network sensitivity to the h_+ and $h_\times$ polarizations respectively.

2.1. Likelihood regulators

As first shown in [4], there is a specific class of constraints (often called regulators), which arise from the way the network responds to a generic GW signal. A classical example is a network of aligned detectors where the detector responses ξ_k are identical. In this case, the algorithm can be constrained to search for an unknown function ξ rather than for two GW polarizations h_+ and $h_\times$, which span a much larger parameter space. Note that in this case $|\mathbf{f}_\times|^2 = 0$, equation (8) is ill-conditioned and the solution for the $h_\times$ waveform cannot be found. The regulators are important not only for aligned detectors, but also for networks of mis-aligned detectors, for example the LIGO and Virgo network [20, 21]. Depending on the source location, the network can be much less sensitive to the second GW component ($|\mathbf{f}_\times|^2 \ll |\mathbf{f}_+|^2$) and the $h_\times$ waveform may not be reconstructed from the noisy data.

In the coherent WaveBurst analysis, we introduce a regulator by changing the norm of the $\mathbf{f}_\times$ vector:

$$|\mathbf{f}'_\times|^2 = |\mathbf{f}_\times|^2 + \delta, \tag{9}$$

where δ is a parameter. This is equivalent to adding one more dummy detector to the network with the antenna patterns $f_{+,K+1} = 0$, $f_{\times,K+1} = \sqrt{\delta}$ and zero detector output ($x_{K+1} = 0$). In this case, the regulator preserves the orthogonality of the vectors $\mathbf{f}_+$ and $\mathbf{f}'_\times$, and the maximum likelihood statistic is written as

$$L_{\max} = \sum_{\Omega_{\rm TF}} \left[\frac{(\mathbf{w}\cdot\mathbf{f}_+)^2}{|\mathbf{f}_+|^2} + \frac{(\mathbf{w}\cdot\mathbf{f}'_\times)^2}{|\mathbf{f}'_\times|^2} \right] = \sum_{\Omega_{\rm TF}} [(\mathbf{w}\cdot\mathbf{e}_+)^2 + (\mathbf{w}\cdot\mathbf{e}'_\times)^2], \tag{10}$$

where $\mathbf{e}_+$ and $\mathbf{e}'_\times$ are unit vectors. Depending on the value of the parameter δ, different statistics can be generated, for example

- $\delta = 0$—standard likelihood,
- $\delta = \infty$—hard constraint likelihood.

2.2. Reconstruction of GW waveforms

GW waveforms are given by the solutions of the likelihood functional equations (5) and (6). For the first GW component, the solution is

$$h_+ = \frac{(\mathbf{w}\cdot\mathbf{f}_+)}{|\mathbf{f}_+|^2}. \tag{11}$$

When the regulator is introduced, it affects the solution for the second GW component. In this case we look for such a solution, which gives the second term of the likelihood statistic $L_{\max}$, when the solution is substituted into the likelihood functional. Namely, we solve the equation

$$2(\mathbf{w}\cdot\mathbf{f}_\times)h_\times - |\mathbf{f}_\times|^2 h_\times^2 - \frac{(\mathbf{w}\cdot\mathbf{f}_\times)^2}{|\mathbf{f}'_\times|^2} = 0. \tag{12}$$

Out of two possible solutions, the following one is selected:

$$h_\times = \frac{(\mathbf{w}\cdot\mathbf{f}_\times)}{|\mathbf{f}'_\times|^2} \left(1 + \sqrt{1 - \frac{|\mathbf{f}_\times|^2}{|\mathbf{f}'_\times|^2}} \right)^{-1}. \tag{13}$$

In the case of aligned detectors ($|f_\times| = 0$), this equation results in a trivial solution $h_\times = 0$.

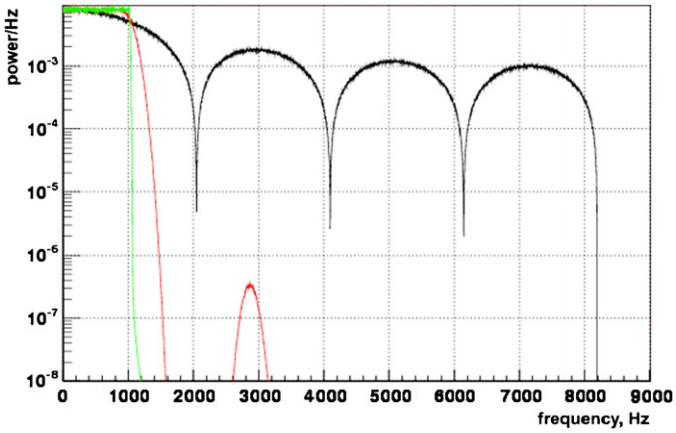

Figure 1. A comparison of spectral leakage from the first (low) frequency band 0–1024 Hz to the high frequency bands for Haar (black), Symlet60 (red) and Meyer1024 (green) wavelets after three wavelet decomposition steps.

3. Data analysis algorithms

In this section, we describe the algorithms used in the coherent WaveBurst pipeline. They include wavelet transformation, conditioning of input data, construction of time delay filters and generation of coherent triggers.

3.1. Wavelet transformation

The discrete wavelet transformations (DWTs) are applied to discrete data and produce discrete wavelet series $w[i, j]$, where j is the scale index and i is a time index. Applied to time series, the DWT maps data from the time domain to the wavelet domain. All DWTs used in cWB have *critical sampling* when the output data vector has the same size as the input data vector.

Wavelet series give a time-scale representation of data where each wavelet scale can be associated with a certain frequency band of the initial time series. Therefore a wavelet time-scale spectra can be displayed as a time-frequency (TF) scallogram, where the scale is replaced with the central frequency f of the band. The time series sampling rate R and the scale number j determine the time resolution $\Delta t_j(R)$ at this scale. The DWT preserves the time-frequency volume of the data samples, which is equal to $1/2$ for the input time series. Therefore, the frequency resolution Δf_j is defined as $1/(2\Delta t_j)$ and determines the data bandwidth at the scale j. For optimal localization of the GW energy on the TF plane, the cWB analysis is performed at several time-frequency resolutions.

The time-frequency resolution defined above should be distinguished from the intrinsic time-frequency resolution of the wavelet transformation, which defines the spectral leakage between the wavelet sub-bands and depends on the length of the wavelet filter. To reduce spectral leakage, we use Meyers wavelets for which long filters can be easily constructed [22]. As shown in figure 1, it allows us much better localization of the burst energy on the time-frequency plane than Symlet60 wavelets used for the LIGO S2-S4 analysis [23, 24]. The disadvantage of the Meyer filters is that for the local support, they have to be truncated. As a result, the Meyer wavelets are approximately orthonormal. From the other side, the Meyer filters can be constructed so that the Parseval identity holds with better than 0.01% accuracy, which is more than adequate for the analysis.

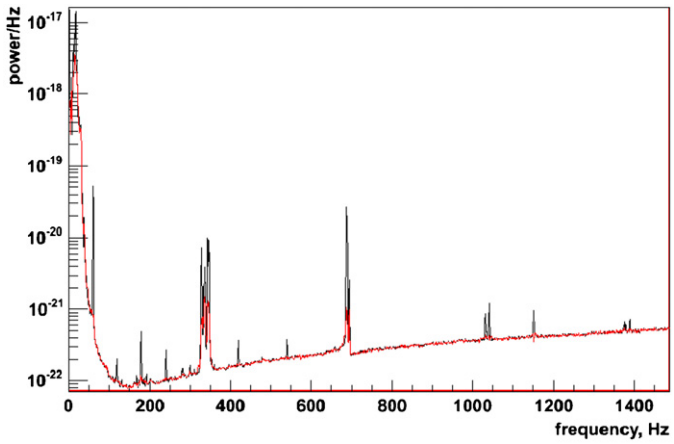

Figure 2. Power spectra of original (black) and LPE filtered (red) noise of the Hanford 4k detector.

3.2. A linear prediction error filter

Linear prediction error (LPE) filters are used to remove 'predictable' components from an input time series. Usually, they are constructed and applied in the time domain. In this case, the output of the LPE filter is a whitened time series. The LPE filters can be also used in the wavelet domain. For construction of the LPE filters, we follow the approach described in [26]. The symmetric LPE filters can be constructed from the backward and forward LPE filters by using the classical Levinson algorithm or the split lattice algorithm.

Since each wavelet layer is a time series, rather than applying the LPE filter to a time series $x(t)$, one can perform a wavelet decomposition $x(t) \to w(f, t)$ first and then construct and apply the LPE filter $F(f)$ individually to each wavelet layer. A set of filters $F(f)$ removes predictable components (like lines) in the wavelet layers producing data $w'(t)$. The filtered time series $x'(t)$ can be reconstructed from $w'(t)$ with the inverse wavelet transformation. An example power spectral density of the filtered segment of S4 data is shown in figure 2. As one can see, when applied in the wavelet domain the LPE filter removes spectral lines but preserves the power spectral density of the noise floor.

3.3. Time delay filters in the wavelet domain

The likelihood method requires calculation of the inner products $\langle x_n(\tau_n), x_m(\tau_m)\rangle$, where the data streams are shifted in time to take into account the GW signal time delay between the detectors n and m. The time delay $\tau_n - \tau_m$ in turn depends on the source coordinates θ and ϕ.

In the time domain, it is straightforward to account for the time delays. However, for colored detector noise, it is preferable to calculate the maximum likelihood statistics in the Fourier or wavelet (time-frequency) domain. In the wavelet domain, one needs to calculate the inner products $\langle w_n(\tau_n), w_m(\tau_m)\rangle$. The delayed amplitudes can be calculated from the original amplitudes (before delay) with the help of the time delay filter $D_{kl}(\tau)$:

$$w_{n,m}(i, j, \tau) = \sum_{kl} D_{kl}(\tau, j) w_{n,m}(i + k, j + l), \tag{14}$$

where k and l are the local TF coordinates with respect to the TF location (i, j). The delay filters are constructed individually for each wavelet layer, which is indicated with the index j.

The construction of time delay filters is related to the decomposition of the sampled wavelet functions $\Psi_j(t + \tau)$ in the basis of the non-shifted wavelet functions $\Psi_j(t)$. The filter

construction procedure can be described in the following steps:

(i) create a wavelet series with only one coefficient at the TF location (i, j) set to unity,
(ii) apply the inverse wavelet transformation reconstructing $\Psi_j(t)$ in the time domain,
(iii) shift $\Psi_j(t)$ by delay time τ and perform wavelet decomposition of $\Psi_j(t+\tau)$,
(iv) the resulting wavelet amplitudes at the TF locations $(i+k, j+l)$ give the delay filter coefficients $D_{kl}(\tau, j)$ for the wavelet layer j.

The length of the filter is determined by the requirement on the acceptable energy loss when the time delay filter is applied. The fractional energy loss is

$$\epsilon_K = 1 - \sum_K D_{kl}^2, \tag{15}$$

where the sum is calculated over the K most significant coefficients. The selected coefficients are also described by the list of their relative TF locations (k, l) which should be stored along with the filter coefficients D_{kl}. Typically, K should be greater than 20 to obtain the fractional energy loss less than 1%.

3.4. Generation of coherent triggers

A starting point of any burst analysis is the identification of burst events (triggers). Respectively, this stage of the burst analysis pipeline is called the event trigger generator (ETG). Usually, ETGs based on the excess power statistics of individual detectors are used in the analyses [16–18]. Another example of an ETG is the CorrPower algorithm [19], which uses cross-correlation between aligned detector pairs to generate the triggers. The likelihood statistic used in the coherent WaveBurst utilizes both the excess power and the cross-correlation terms.

3.4.1. Likelihood time-frequency maps. In general, the likelihood functional is calculated as a sum over the data samples selected for the analysis (see equation (1)). The number of terms in the sum depends on the selected TF area in the wavelet domain. When the sum consists of only one term, one can write the likelihood functional for a given TF location and point in the sky[3]:

$$\mathcal{L}_p(i, j, \theta, \phi) = |\mathbf{w}|^2 - |\mathbf{w} - \mathbf{f}_+ h_+ - \mathbf{f}_\times h_\times|^2. \tag{16}$$

Since the entire likelihood approach is applicable to the above functional, one can solve the variation problem and find the maximum likelihood statistics $L_p(i, j, \theta, \phi)$. They can be maximized over the source coordinates θ and ϕ, resulting in the statistics

$$L_m(i, j) = \max_{\theta,\phi}\{L_p(i, j, \theta, \phi)\}. \tag{17}$$

Calculated as a function of time and frequency, it gives a likelihood time-frequency (LTF) map. Figure 3 shows an example of the LTF map for a segment of the S4 data.

A single data sample in the map is called the LTF pixel. It is characterized by its TF location (i, j) and by the arrays of wavelet amplitudes $w_k(i, j, \tau_k(\theta, \phi))$, which are used to construct the likelihood statistics L_p.

3.4.2. Coherent triggers. The statistic L_m has a meaning of the maximum possible energy detected by the network at a given TF location. By selecting the values of L_m above some threshold, one can identify groups of the LTF pixels (coherent trigger) on the time-frequency plane. A coherent trigger is defined for the entire network, rather than for the individual

[3] For definition of vectors $\mathbf{w}$, $\mathbf{f}_+$ and $\mathbf{f}_\times$, see equations (3) and (4).

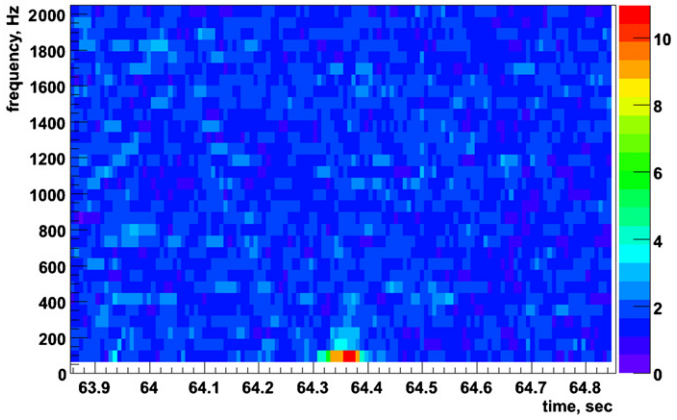

Figure 3. Example of the likelihood time-frequency map for a magnetic glitch in the S4 L1xH1xH2 data.

detectors. Therefore, further in the text we reserve a name 'cluster' for a group of pixels selected in a single detector and refer to a group of the LTF pixels as a coherent or network trigger.

After the coherent triggers are identified, one has to reconstruct the parameters of the GW bursts associated with the triggers, including the reconstruction of the source coordinates, the two GW polarizations, the individual detector responses and the maximum likelihood statistics of the triggers. The likelihood of coherent triggers is calculated as

$$\mathcal{L}_c(\theta, \phi) = \sum_{ij} \mathcal{L}_p(i, j, \theta, \phi), \tag{18}$$

where the sum is taken over the LTF pixels in the trigger. The maximum likelihood statistic $L_{\max}$ is obtained by variation of L_c. Unlike for L_p, which is calculated for a single LTF pixel, $L_{\max}$ is calculated simultaneously for all LTF pixels forming the coherent trigger.

4. Selection of coherent triggers

When the detector noise is Gaussian and stationary, the maximum likelihood $L_{\max}$ is the only statistic required for detection and selection of GW events. In this case, the false alarm and the false dismissal probabilities are controlled by the threshold on $L_{\max}$. The real data, however, are contaminated with the instrumental and environmental glitches and additional selection cuts should be applied to distinguish genuine GW signals [6, 25]. Such selection cuts test the consistency of the reconstructed responses in the detectors. In the coherent WaveBurst method, the consistency test is based on the coherent statistics constructed from the elements of the likelihood and the null matrices.

The likelihood matrix L_{nm} is obtained from the likelihood quadratic form (see equation (10)):

$$L_{\max} = \sum_{nm} L_{nm} = \sum_{nm} [\langle w_n w_m e_{+n} e_{+m} \rangle + \langle w_n w_m e'_{\times n} e'_{\times m} \rangle]. \tag{19}$$

where n and m are the detector indices. The diagonal (off-diagonal) terms of the matrix L_{mn} describe the reconstructed normalized incoherent (coherent) energy. The sum of the

off-diagonal terms is the coherent energy $E_{\rm coh}$ detected by the network. The coherent terms can be used to construct the correlation coefficients:

$$r_{nm} = \frac{L_{nm}}{\sqrt{L_{nn}L_{mm}}}, \tag{20}$$

which represent Pearson's correlation coefficients in the case of aligned detectors. We use the coefficients r_{nm} to construct the reduced coherent energy

$$e_{\rm coh} = \sum_{nm} L_{nm}|r_{nm}|, \qquad n \neq m, \tag{21}$$

which provides one of the most efficient selection cuts for rejection of the incoherent background events.

The null matrix represents the normalized energy of the reconstructed noise

$$N_{nm} = E_{nm} - L_{nm}, \tag{22}$$

where E_{nm} is the diagonal matrix of the normalized energy in the detectors: $E_{nn} = \langle x_n^2 \rangle$. To distinguish genuine GW signals from the instrumental and environmental glitches, we introduce the network correlation coefficients

$$C_{\rm net} = \frac{E_{\rm coh}}{N_{\rm ull} + |E_{\rm coh}|}, \qquad c_{\rm net} = \frac{e_{\rm coh}}{N_{\rm ull} + |e_{\rm coh}|}, \tag{23}$$

where $N_{\rm ull}$ is a sum of all elements of the null matrix, which represents the total energy in the null stream. Usually, for glitches, little coherent energy is detected and the reconstructed detector responses are inconsistent with the detector outputs which result in the large null energy. Therefore, the correlation coefficients $C_{\rm net}$ and $c_{\rm net}$ can be used for a signal consistency test which effectively compares the null energy with the coherent energy. This is a much safer consistency test than the null stream veto [25], where the null energy is compared with the estimated noise energy. In any realistic data analysis, there is always some residual energy left in the null stream. Therefore, for strong gravitational waves the energy of the residual signal can be much larger than the noise energy, that may result in the false rejection of the GW signals. This is not the case for the consistency tests based on $C_{\rm net}$ and $c_{\rm net}$.

5. Summary

In the paper, we discussed how the coherent network algorithms are constructed for burst searches. We found it convenient to construct coherent burst searches in the time-frequency (wavelet) domain, which requires the construction of time delay filters. For detection of burst signals, we combine the output of all detectors into one coherent statistic—likelihood—which represents the total signal-to-noise ratio of the signal detected in the network. To distinguish genuine GW signals from the instrumental and environmental glitches, we introduced several coherent statistics constructed from the elements of the likelihood and null matrices. We do not discuss the performance of the method in this paper; however, numerous studies of the method with different sets of real LIGO and Virgo data have been performed. It was found, in general, that the method has better performance than the burst algorithm used for the published analysis of the LIGO data [16, 20, 21]. The results of these studies will be presented in subsequent papers.

Acknowledgments

We thank Keith Riles, Michele Zanolin and Brian O'Reilly for detailed discussions and review of the algorithm and suggestions which significantly improved its performance. This work

was supported by the US National Science Foundation grant PHY-0555453 to the University of Florida, Gainesville, Florida.

References

[1] Gursel Y and Tinto M 1989 *Phys. Rev.* D **40** 3884
[2] Flanagan E E and Hughes S A 1998 *Phys. Rev.* D **57** 4577
[3] Arnaud N *et al* 2003 *Phys. Rev.* D **68** 102001
[4] Klimenko S, Mohanty S, Rakhmanov M and Mitselmakher G 2005 *Phys. Rev.* D **72** 122002
[5] Rakhmanov M 2006 *Class. Quantum Grav.* **23** S673
[6] Chatterji S *et al* 2006 *Phys. Rev.* D **74** 082005
[7] Zwerger T and Mueller E 1997 *Astron. Astrophys.* **320** 209
[8] Dimmelmeier H, Font J A and Mueller E 2002 *Astron. Astrophys.* **393** 523
[9] Ott C *et al* 2004 *Astrophys. J.* **600** 834
[10] Shibata M and Sekiguchi Y I 2004 *Phys. Rev.* D **69** 084024
[11] Flanagan E E and Hughes S A 1998 *Phys. Rev.* D **57** 4535
[12] Baker J *et al* 2006 *Phys. Rev.* D **73** 104002
[13] Pretorius F 2005 *Phys. Rev. Lett.* **95** 121101
[14] Campanelli M *et al* 2006 *Phys. Rev. Lett.* **96** 111101
[15] Meszaros P 2006 *Rep. Prog. Phys.* **69** 2259–322
[16] Klimenko S and Mitselmakher G 2004 Wavelet method for GW burst detection *Class. Quantum Grav.* **21** S1819
Klimenko S and Mitselmakher G 2004 *Class. Quantum Grav.* **21** S1685
[17] Chatterji S, Blackburn L, Martin G and Katsavounidis E 2004 Multiresolution techniques for the detection of gravitational-wave bursts *Class. Quantum Grav.* **21** S1809
[18] McNabb J W C *et al* 2004 *Preprint* gr-qc/0404123v1
[19] Cadonati L 2004 Coherent waveform consistency test for LIGO burst candidates *Class. Quantum Grav.* **21** S1695
[20] Abbott B *et al* (The LIGO Scientific Collaboration) 2006 *Class. Quantum Grav.* **23** S51–6
[21] Acernese F *et al* (The Virgo Collaboration) 2006 *Class. Quantum Grav.* **23** S63–9
[22] Vidakovic B 1999 *Statistical Modeling by Wavelets* (New Work: Wiley)
[23] Abbot B *et al* 2005 *Phys. Rev.* D **72** 062001
[24] Abbot B *et al* 2007 *Class. Quantum Grav.* **24** 5343–69
[25] Wen L and Schutz B F 2005 Coherent network detection of gravitational waves: the redundancy veto *Class. Quantum Grav.* **22** S1321
[26] Delsarte P and Genin Y 1987 *On the Splitting of Classical Algorithms in Linear Prediction Theory* (Piscataway, NJ: IEEE) ASSP-35